Regular Article

PHYSICAL CHEMISTRY RESEARCH
Published by the
Iranian Chemical Society
www.physchemres.org
info@physchemres.org

Phys. Chem. Res., Vol. 10, No. 4, 537-547, December 2022
DOI: 10.22036/PCR.2022.326878.2023

Effect of PVA/PEG-coated Fe_3O_4 Nanoparticles on the Structure, Morphology and Magnetic Properties

A. Khodadadi[a], M.R. Talebtash[b] and M. Farahmandjou[c,*]

[a]*Department of Physics, Tehran North Branch, Islamic Azad University, Tehran, I. R. Iran*
[b]*Department of Engineering Shahriar, Branch Islamic Azad University, Shahriar, Iran*
[c]*Departments of Physics, Varamin Pishva Branch, Islamic Azad University, Varamin, Iran*

(Received 16 November 2021, Accepted 3 March 2022)

Iron oxide (Fe_3O_4) nanoparticles (NPs) are the most important group of magnetic nanoparticles. In this study, iron oxide (Fe_3O_4) magnetic nanoparticles (MNPs) were modified by polyethylene glycol (PEG) and polyvinyl alcohol (PVA) coating co-precipitation method. MNPs were characterized by XRD, FTIR, TEM, DLS, and VSM analyses to study their structure, morphology, and magnetic properties. The results showed the superior properties of PEG and PVA-coated Fe_3O_4 compared to the pristine sample. It was found that modified Fe_3O_4 MNPs improved the magnetic saturation. The estimated particle size of PEG-coated Fe_3O_4 nanoparticles was 11 nm with magnetic saturation of 60.98 emu g^{-1} and coercivity of 8.26G.

Keyword: Fe_3O_4 nanoparticles, PVA/PEG coating, Superparamagnetic, Co-precipitation method

INTRODUCTION

Iron oxide (Fe_3O_4) nanoparticles (NPs) have desirable physical and chemical properties and provide valuable capabilities for many applications. Researchers are increasingly considering these NPs depending on their morphology, size, and magnetic saturation. Magnetic Nanoparticles (MNPs) have been received significant attention because of their excellent compatibility, superparamagnetic properties, and high specific surface area [1-5]. Magnetic nanoparticles can be separated easily by an external magnetic field due to their high magnetic capacity. This is useful in various fields, such as producing advanced medical materials, energy and membrane production materials, electricity generation, construction of data storage devices, medical engineering, magnetic resonance imaging, and optical and microwave magnetic devices [6-12]. Also, their dispersibility in water and superparamagnetic properties led to important use of these compounds in biological fields [13]. Magnetite Fe_3O_4 and maghemite γ-Fe_3O_4 are the two main structural forms of this kind of MNP. Among the mentioned structures, magnetite has better magnetic saturation than the other [14]. There are various methods for the synthesis of magnetic nanoparticles: mechanical crushing methods as well as chemical methods such as co-precipitation, hydrothermal, sonochemistry, electrochemical deposition, solvothermal, and microemulsion [15-19]. Among these methods, the co-precipitation method is more suitable due to its simplicity, high efficiency, low production cost, short reaction time, low-temperature process, production of high purity particles, and the use of an aqueous environment [20,21]. Therefore, it is a more common and beneficial method than the other similar methods. In this research, all the experiments have been performed based on the more desirable co-precipitation method. The MNPs are unstable after synthesizing; they tend to be agglomerated as the electrostatic attraction tends to reach a lower energy level while undergoing the synthesis process and drying. In

*Corresponding author. E-mail: majidfarahmandjou@gmail.com

addition, changing the oxidation state from Fe^{2+} to Fe^{3+} in the atmospheric environment diminishes the formational magnetite quality [22]. Coating the nanoparticles using polymeric and mineral agents is very essential to prevent the agglomeration of nanoparticles [23,24].

In 2007, Liu *et al*. synthesized magnetic nanoparticles using silica and sol-gel method [25]. They investigated the effects of ethanol, ammonium, and tetraethyl *ortho*-silica solution on the morphology, magnetic properties, and particles distribution. The saturation magnetization of the coated magnetic nanoparticles was calculated to be less than 20 emu g^{-1}. This coating was heavy and caused problems in the dispersion process. Businova and co-workers fabricated iron oxide nanoparticles using emulsion (polymerization method); they determined the size of the magnetic nanoparticles to be 20 nm [26]. An electrochemical method was used to synthesize magnetic nanoparticles by Karimzadeh *et al*.; they applied $FeCl_3.6H_2O$ precursor and two polymeric agents, polyethylene amine and polyethylene glycol (PEG) polymer, in their research. However, the amount of saturation magnetization of the nanoparticles was 32 emu g^{-1}. This high-power consumption was a problem for applying this method in the industrial applications [27].
In another method, $FeCl_3.6H_2O$, sodium acetate, and PEG polymer agents were used to modify MNPs using hydrothermal method by Ani *et al*. They synthesized both Fe_3O_4 and maghemite phase (γ-Fe_2O_3) in this synthesis method with a size of 20 nm. However, no further study has been performed on other structural and magnetic properties [28]. In 2016, magnetic nanoparticles, namely ferrous chloride-tetrahydrate, ferric chloride-hexahydrate, ammonium solution, and polymer agent TEOS (Tetra ethoxy silane), were synthesized by Hassanzadeh *et al*. using co-precipitation method; they reported saturation magnetization of 58.5 emu g^{-1} [29]. Although the process was performed under an inert atmosphere of nitrogen to prevent oxidation, the coating agent did not encompass the nanoparticle surface. Also, the polymeric agent was heavy and caused problems in the dispersion process. The size of nanoparticles was 40 nm. In 2020, Antarnusa *et al*. used magnetic nanoparticles in biosensors and coated them with PEG at different concentrations. They synthesized coated magnetic nanoparticles by co-precipitation method and used $FeCl_3.6H_2O$ and $FeSO_4.7H_2O$ ammonium solution and PEG. The maximum saturation magnetization that they found was 60 emu g^{-1}. By applying 3g PEG, the amount of saturation magnetization was about 40 (emu g^{-1}) [30,31]. The different phases of MNPs were formed in this method due to synthesis in the atmospheric conditions. In 2019, Maleki *et al*. used a polyvinyl alcohol (PVA) coating agent to modify and optimize the surface of the iron oxide by nanoparticles-precipitation method. To synthesize nanoparticles, they used ferrous chloride tetrahydrate, ferric chloride hexahydrate, and ammonia solution. The determined saturation magnetization was about 32 emu g^{-1}, and the calculated size of the NPs was about 47 nm [32].
Meanwhile, the co-precipitation method has become more popular because of the morphology of the particles and outstanding magnetic properties. In this study, magnetite Fe_3O_4 nanoparticles were modified by two PEG and PVA coating agents, and alkaline agent NH_4OH at low and high temperatures. The nanoparticles' structural, morphological, optical, dynamic, and magnetic properties are evaluated.

MATERIALS

Ferrous chloride tetrahydrate (99%), ferric chloride hexahydrate (99%), ammonia solution (25%), chloric aside (37%), distilled water, polyethylene glycol 4000 (PEG-1000), and polyethylene glycol (PVA) were used to synthesize the pure and coated magnetic nanoparticles. Equipment included a digital scale with an accuracy of 0.0001 g with the model KF3004, Hidolph magnetic stirrer HEI-TEC0145, Electrothermal EM1000CE, HANNA digital PH meter Hi 2211, an oven BM120E, and a digital thermometer STC-100A.

EXPERIMENTS AND METHOD

Pure and coated Fe_3O_4 magnetic nanoparticles were fabricated using the co-precipitation method with $FeCl_3.6H_2O$ and $FeCl_2.4H_2O$ precursors and modified by the two different PEG and PVA polymer agents. Pure samples were synthesized by mixing 2.7 g ferric chloride hexahydrate ($FeCl_3.6H_2O$) and 1 g ferrous chloride tetrahydrate ($FeCl_2.4H_2O$) in a 2:1 ratio in a three-necked flask. Then, 15 ml hydrochloric acid (0.5 M) was added and stirred at 300 rpm. At 70 °C, this mixed solution was

deoxygenized by nitrogen gas for 20 min. In another flask, ammonium solution (2 M) was deoxygenated under nitrogen gas for 20 min. Then the mixed solution was added dropwise to the alkaline solution until a black nanoparticle appeared by adding any drop and formed a suspension magnetic nanoparticle at a pH = 12. By using an external magnetic field, MNPs were separated from the solution. After washing several times with deionized water, PH reached 7. In this case, the product was dried at 50 °C by an oven. The chemical equation to produce Fe_3O_4 is expressed as follows (Eqs. (1) and (2)).

$$Fe^{2+} + 2Fe^{3+} + 8OH^- \rightarrow Fe(OH)_2 + 2Fe(OH)_3 \quad (1)$$

$$Fe(OH)_2 + 2Fe(OH)_3 \rightarrow Fe_3O_4 + 4H_2O \quad (2)$$

For preparing coated MNPs, a mixture of $FeCl_3.6H_2O$, $FeCl_2.4H_2O$ (2:1), and 3 g PEG were first prepared in a three-necked flask, then dissolved in 15 ml hydrochloric acid (0.5 M) under a magnetic stirrer at 300 rpm. Simultaneously, ammonium solution (2 M) was prepared in another flask, and both were immersed under nitrogen atmospheric conditions for 20 min. Then the mixture was added dropwise to the ammonium solution (2 M). Ultimately, black nanoparticles were gradually formed. Suspension of magnetic nanoparticles was separated from the solution by an external magnetic field at a pH of about 12. The resulting product was washed several times with pure water to reach a neutral pH (pH = 7). Afterward, it was dried inside the oven at 50 °C. In the next step, 0.5 g of PVA polymer agent was used instead of PEG to prepare the coated MNPs (as shown in Fig. 1). The obtained powders were characterized for further study by XRD, DLS, SEM, TEM, FTIR, and VSM analyses.

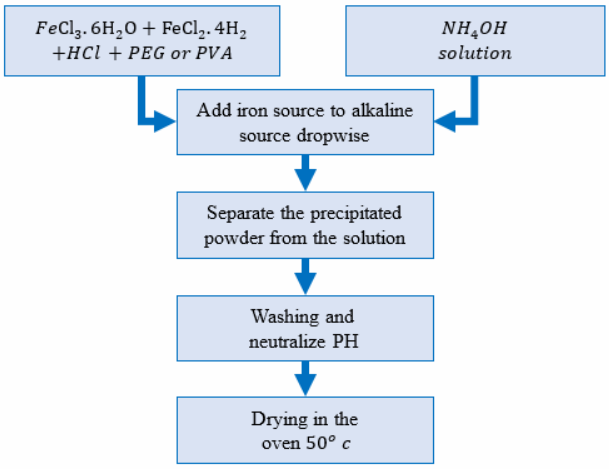

Fig. 1. Schematic synthesis of MNPs.

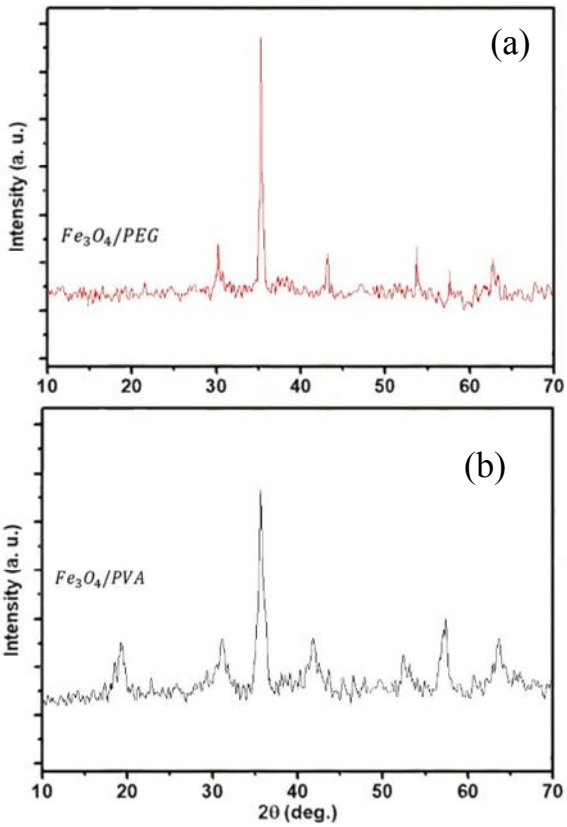

Fig. 2. XRD spectrum of (a) Fe_3O_4/PEG and (b) Fe_3O_4/PVA magnetic nanoparticles.

RESULTS AND DISCUSSIONS

Table 1 compares different methods and magnetic properties of Fe_3O_4 synthesized with different coating agents. As illustrated, the precursors and co-precipitation methods were more suitable than other methods for MNPs synthesis. In this case, the modified MNPs had better magnetic properties and smaller sizes. In addition, the mentioned properties demonstrated the more improvement when using the PEG coating agent.

Figure 2 shows the x-ray diffraction (XRD) analysis of

Table 1. Comparison of Methods and Results of Fe_3O_4 Synthesis with Different Coating Agents

Method	Materials used	Coating agent	Size (nm)	M_s (emu g^{-1})	H_c (Oe)	Atmosphere	Complexity and process time	Ref.
Sol-gel	TEOS, NH_3, $FeCl_3.6H_2O$ $FeCl_2.4H_2O$ distilled water	tetraethyl *ortho*-silica	12	25	-	Air	Several steps - long time	[16]
Electrochemical	$FeCl_3.6H_2O$, $FeCl_2.4H_2O$, distilled water	Polyethylene amine, PEG	10	32.5	1.25	Air	Several steps - long time	[18]
Hydrothermal	$FeCl_3.6H_2O$, $FeCl_2.4H_2O$, Sodium Acetate, distilled water	PEG	20	-	-	Air	Several steps - long time	[19]
Co-precipitation	$FeSO_4.7H_2O$, $FeCl_3.6H_2O$, NH_4OH distilled water.	PEG (3 g)	10	40	50	Air	Several steps - long time	[20]
Emulsion	$FeCl_3.6H_2O$, $FeCl_2.4H_2O$, H_2SO_4 TMAOH, distilled water	Methyl methoxylated	~20	-	-	Air	Several steps - long time	[17]
Co-precipitation	$FeCl_2{\cdot}4H_2O$, NH_4OH, distilled water	PVA	47	32	-	Nitrogen	Several steps - long time	[21]
In situ Co-precipitation	$FeCl_3.6H_2O$, $FeCl_2.4H_2O$, HCL, NH_4OH, distilled water	PEG (3 g)	10	60.94	8.28	Nitrogen	On-site coverage - shorter time - better efficiency	This work
	$FeCl_3.6H_2O$, $FeCl_2.4H_2O$, HCL, NH_4OH, distilled water	PVA	20	32.39	8.38	Nitrogen		

Method	Materials used	Coating agent	Size (nm)	M_s (emu g^{-1})	H_c (Oe)	Atmosphere	Complexity and process time	Ref.
Sol-gel	TEOS, NH_3, $FeCl_3.6H_2O$ $FeCl_2.4H_2O$ distilled water	tetraethyl *ortho*-silica	12	25	-	Air	Several steps - long time	[16]
Electrochemical	$FeCl_3.6H_2O$, $FeCl_2.4H_2O$, distilled water	Polyethylene amine, PEG	10	32.5	1.25	Air	Several steps - long time	[18]
Hydrothermal	$FeCl_3.6H_2O$, $FeCl_2.4H_2O$, Sodium Acetate, distilled water	PEG	20	-	-	Air	Several steps - long time	[19]
Co-precipitation	$FeSO_4.7H_2O$, $FeCl_3.6H_2O$, NH_4OH distilled water.	PEG (3 g)	10	40	50	Air	Several steps - long time	[20]
Emulsion	$FeCl_3.6H_2O$, $FeCl_2.4H_2O$, H_2SO_4 TMAOH, distilled water	Methyl methoxylated	~20	-	-	Air	Several steps - long time	[17]
Co-precipitation	$FeCl_2{\cdot}4H_2O$, NH_4OH, distilled water	PVA	47	32	-	Nitrogen	Several steps - long time	[21]
In situ Co-precipitation	$FeCl_3.6H_2O$, $FeCl_2.4H_2O$, HCL, NH_4OH, distilled water	PEG (3 g)	10	60.94	8.28	Nitrogen	On-site coverage - shorter time - better efficiency	This work
	$FeCl_3.6H_2O$, $FeCl_2.4H_2O$, HCL, NH_4OH, distilled water	PVA	20	32.39	8.38	Nitrogen		

coated (Fe_3O_4/PEG) nanoparticles. The sample's crystal structure, phases, and particle size were studied by XRD analysis at room temperature. As it is clear in the XRD images, the crystal structure of PEG-coated magnetic nanoparticles was similar to the pure magnetic nanoparticles. The MNP structure remained unchanged during the coating with PEG. The crystal structure was "face center cubic (FCC)," and the molecular structure was "inverse spinel," with a lattice constant of 8.346 Å and unit cell. No impurity phases were observed in the spectrum. The positions and relative intensities of the strong diffraction peaks were located at angles 2θ = 30/2° (220), 35/4° (311), 43/1° (400), 53/4° (422), 57/5° (511), and 62/7° (440). These data correspond well to the magnetite-related values according to the JCPS-19629 card number. The Peaks confirm the presence of a magnetic crystal structure of magnetite with cubic spinel structure as a dominant factor in the synthesis of coated nanoparticles. The kind and distribution of the cations at quadrilateral and octahedral sites of the spinal structure significantly affect the magnetic properties of MNPs. The sample's good crystallinity and high purity indicate the proper synthesis method that used. The size of the nanoparticle was calculated by Scherer's Eq. (2) using reference peak specifications (311) [33]. The crystallite size of coated MNPs was about 11 nm.

$$d = \frac{0.9\lambda}{\beta \cos\theta} \tag{2}$$

As can be seen, MNPs growth prevention and nanoparticles size-reduction are direct consequences of coating the PEG polymer agent on the surface of the magnetic nanoparticles.

Figure 2b shows the XRD analysis of the nanoparticles with PVA (Fe_3O_4/PVA). The peaks generated in the XRD spectrum indicate the presence of two magnetic and amorphous phases. The lattice parameters' values of Fe_3O_4 in the sample were a = b = c = 8.365 Å. This study also determined the crystal structure of MNPs in this cube spinel. The Fe^{3+} cations occupied all tetrahedral sites in the sample structure, and the Fe^{2+} cations occupied half of the octahedral sites in the Fe_3O_4 crystal structure. The distribution of these metal ions determines the magnetic torque Fe_3O_4, showing that the magnetic moment between the ions at the tetrahedral and octahedral sites was also opposite. The intense peaks at angles 2θ = 31.17°, 35.5°, 43.5°, 52.5°, 57.4°, and 63.16°, were related to the (220), (311), (400), (422), (511), and (440) planes of Fe_3O_4, respectively. Additionally, the amorphous phase diffraction peak was found at an angle of 2θ = 19.2°. This peak confirms the existence of PVA in the sample. According to the JCPS-65-3107 card number, it represented a cubic spinel structure. The size of the modified MNPs was determined at about 19 nm, according to Scherrer's Eq. (2).

It is clear that the polymeric agent affects the growth phase of the nanoparticles and reduces the size of the nanoparticles by the inhibiting growth. FTIR analysis was used to determine the functional group and vibrational bonds in pure samples and samples coated with two different polymers PEG and PVA. The transmission spectra of the samples were examined in the wavenumber range of 400-4000 cm^{-1}. Figure 3 represents the FTIR analysis of pure MNPs, polymer agent PEG, and MNPs coated with the PEG polymer agent. Accordingly, the absorption bands in the regions of 874.2 cm^{-1} to 1384.4 cm^{-1} were absent in the spectrum of the pure magnetic nanoparticles Fe_3O_4, while these bonds were present in the PEG polymer agent spectrum. The presence of these bands in the spectrum of coated MNPs indicates the replacement of PEG on the surface of MNPs. The peaks at a frequency of 1627.0 cm^{-1}

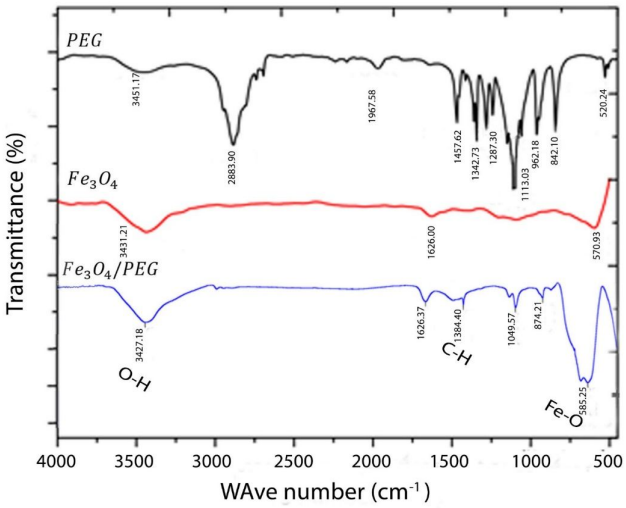

Fig. 3. FTIR analysis of PEG and pure Fe_3O_4 and Fe_3O_4/PEG samples.

were attributed to the bending vibration of the water absorption from the surface of Fe_3O_4 magnetic nanoparticles. The results of the PEG-coated sample also revealed that the absorption peak at the wavenumber 3451.1 cm^{-1} was related to the tensile -OH band, the frequency of 1467 cm^{-1} was associated with the bending band of C-OH, and the frequency of 1113 cm^{-1} corresponded to the tensile band C-O-C [27,34].

Similarly, Fig. 4 shows the FTIR spectra of the PVA, Fe_3O_4, and Fe_3O_4/PVA synthesized nanoparticles. Comparison of the FTIR spectra of samples with each other indicates the placement of the polymeric agent on the MNPs. The strong absorption peak in the wavenumber of 1111.81 cm^{-1} was related to the vibration band of Fe-O-C [28,29,35], showing the placement of the PVA polymer agent on the surface of the Fe_3O_4 nanoparticles. Furthermore, it indicated the interaction between the polymer agent and magnetite nanoparticles. The absorption peak at the frequency of 3364.2 cm^{-1} was attributed to the vibrating banner O-H. A strong absorption band at 2879.4 cm^{-1} indicated an asymmetric tensile vibration in the C-H groups.

DLS analysis was used to determine the size of coated magnetic nanoparticles with PEG and PVA polymer agents. According to the diagram in Fig. 5, the average size of nanoparticles synthesized with PEG and PVA coating agent was reported at 10 nm and 20 nm, respectively. The results were in agreement with the values obtained in the XRD analysis. Due to the average nanoparticle size around 20 nm, it can be concluded that the synthesized nanoparticles were not agglomerated.

TEM analysis was used to determine the exact size of MNPs. For this purpose, the nanoparticle powder was dissolved in the desired solvent and then placed on the copper grades. Figure 6 shows the TEM analysis of MNPs coated with two different polymers. Based on this Figure, the shapes of the nanoparticles were almost spherical, and they were somewhat attached, which was due to the electrostatic repulsion and steric hindrance force [36,37]. The determined mean size of superparamagnetic nanoparticles coated with PEG and PVA were 11 nm and 20 nm, respectively.

The magnetic properties of the coated MNPs in different conditions were studied by VSM analysis [4,38]. The

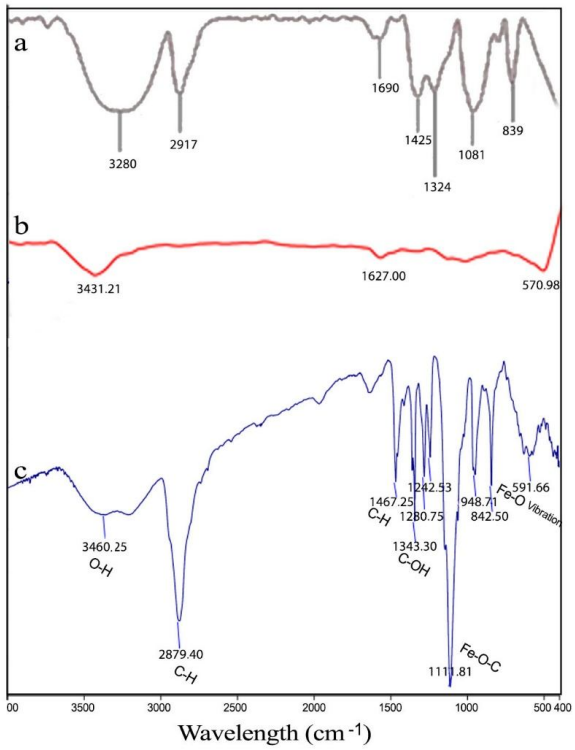

Fig. 4. FTIR analysis of (a) PVA, (b) Fe_3O_4, and (c) Fe_3O_4/PVA samples.

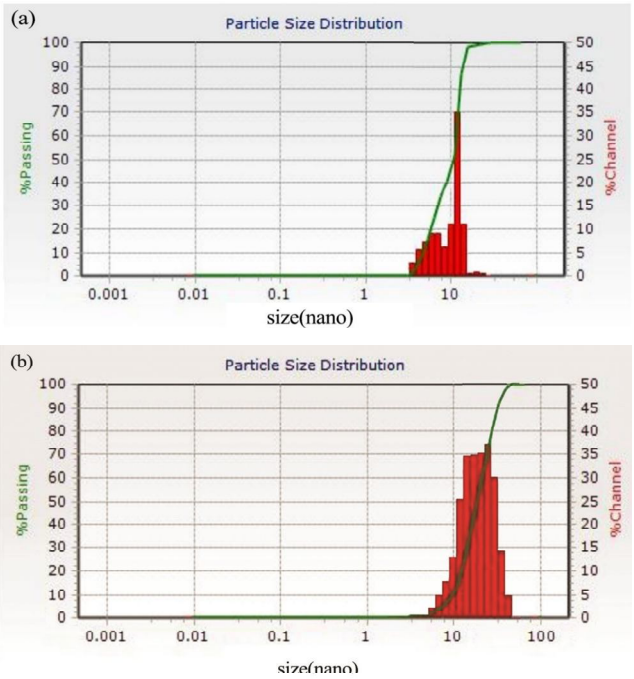

Fig. 5. DLS spectrum of magnetic nanoparticles coated with (a) PEG- (b) PVA- coated Fe_3O_4.

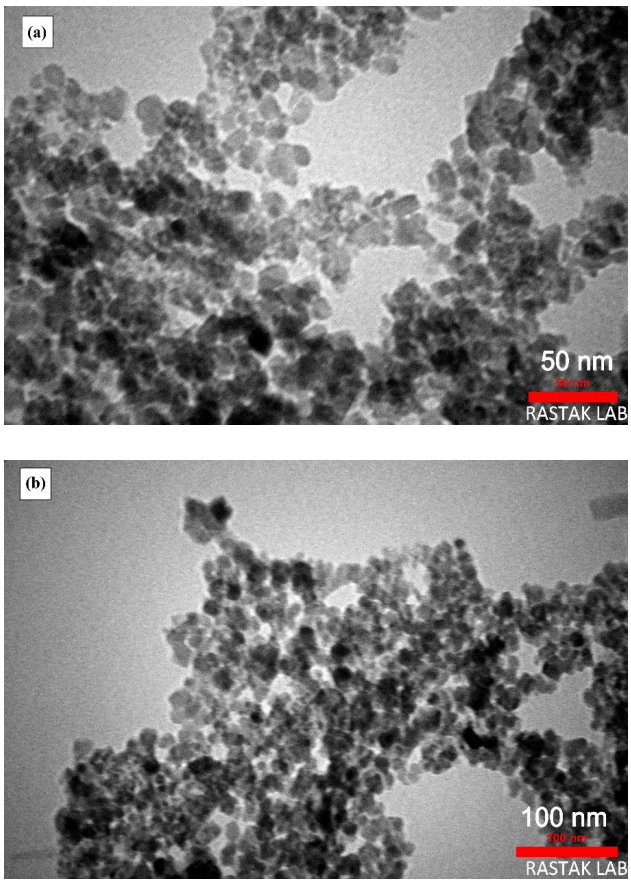

Fig. 6. TEM analysis (a) Fe_3O_4/PEG and (b) Fe_3O_4/PVA magnetic nanoparticles.

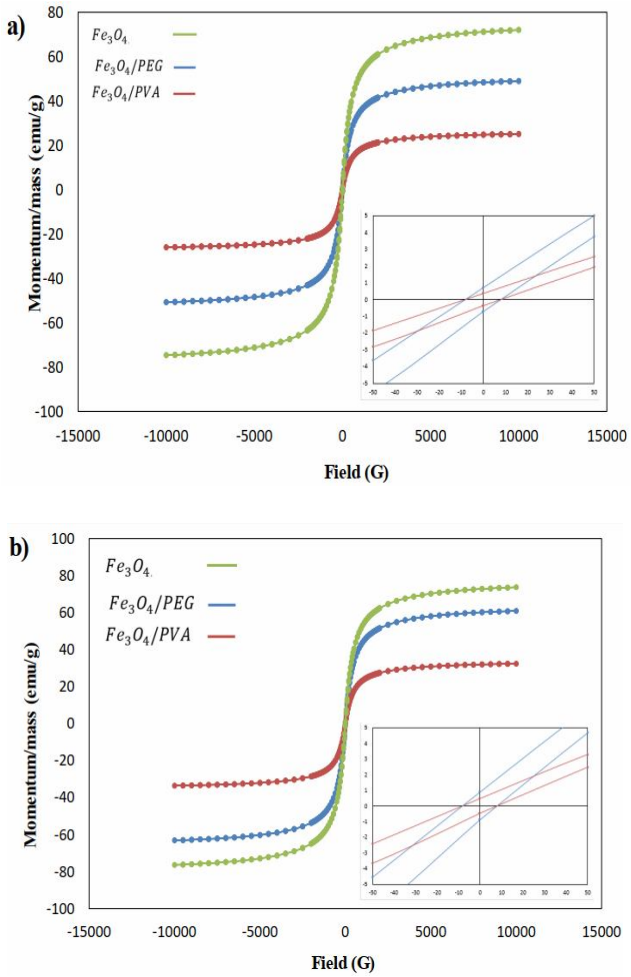

Fig. 7. VSM analysis of Fe_3O_4/PEG and Fe_3O_4/PVA particles at (a) 20 °C and (b) 80 °C.

amount of the saturation magnetism, magnetic remanent, and coercive force of each sample was analyzed and compared. This analysis showed that magnetic nanoparticles exhibited superparamagnetic properties [38-44]. The results proved that the magnetic saturation and coercivity were approximately 60.98 emu g^{-1} and 8.26 G, respectively, for the PEG-coated Fe_3O_4 sample. Figure 7 shows the hysteresis diagram of pure magnetic nanoparticles and modified sample with the two polymeric agents, PEG and PVA, at 20 and 80 °C. As illustrated, the amount of saturation magnetism of coated MNPs with PEG was higher than that of PVA-modified samples. The inset showed the magnetic behavior of the two modified samples at 20 °C and 80 °C.

Further, the synthesis of MNPs with the two coating agents PEG and PVA was performed at low and high temperatures. The amount of saturated magnetization was significantly higher for the PEG coating sample (Fig. 8). Due to the reduced crystal size of the nanoparticles and the presence of a diamagnetic shell that encapsulated the magnetic nanoparticles, the saturated magnetization of the modified MNPs was less than the pure one [25-28]. The results also showed the positive correlation between the temperature and the magnetic saturation of the coated magnetic nanoparticles as increasing of the former (below the Curie temperature) enhanced the latter. This is due to the fact that at high temperatures, the coupling of magnetic moments is better than at low temperatures. Figure 8a indicates the quantities obtained from this investigation. Figure 8b shows the modified samples' small amounts of

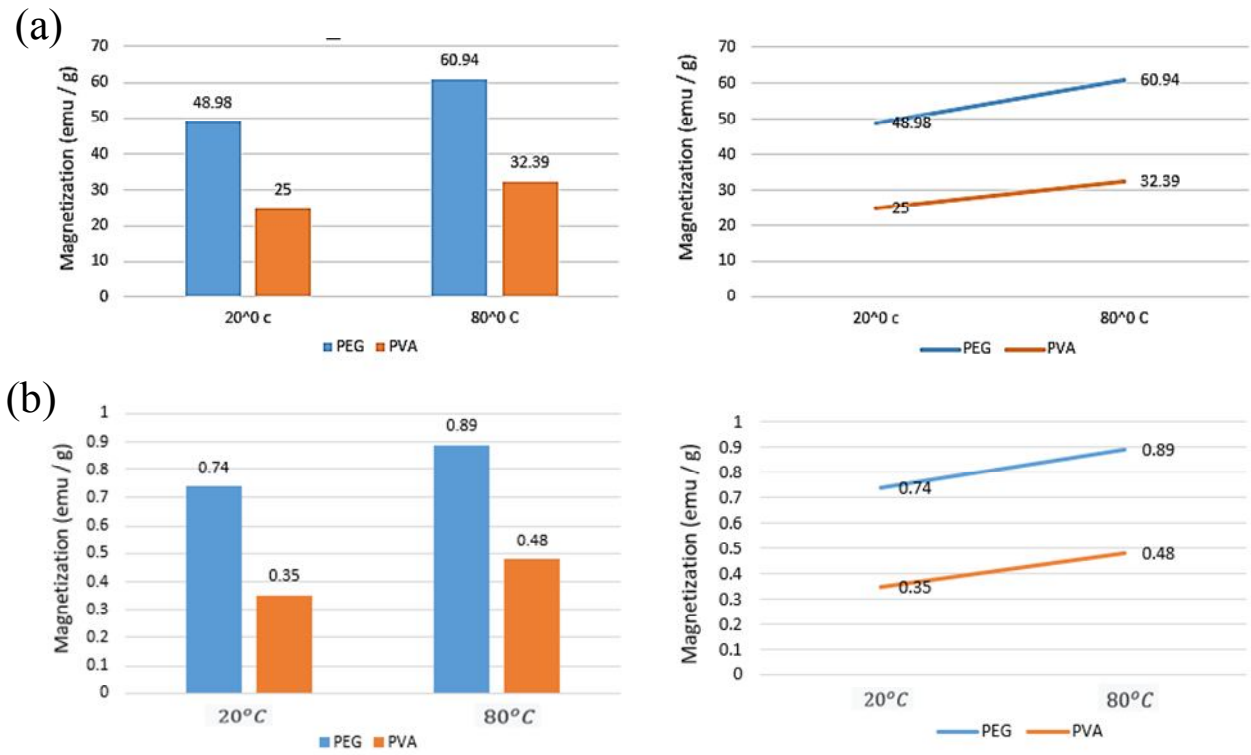

Fig. 8. (a) Effect of coating agent and temperature on magnetization (b) Normalized magnetic remanent of the PEG- and PVA-coated Fe_3O_4 MNPs at different temperatures.

magnetic remanent at both low and high temperatures. The amount of magnetic remanent of the modified MNPs increased slightly with an increase in temperature. The results showed that the both samples had superparamagnetic behavior.

CONCLUSIONS

In conclusion, PEG- and PVA- coated Fe_3O_4 MNPs were successfully synthesized by the co-precipitation method. The PEG and PVA coating samples significantly affected the morphology of the MNPs, stabilized and reduced the particle size. High-temperature synthesis played a crucial effect in the magnetic properties of the MNPs. Comparison the two polymeric agents showed that the PEG was more suitable than the PVA for stabilizing the morphology and for the better magnetic properties. According to the results, PEG coating samples can be used in biomedical fields, such as targeted drug delivery and biomolecular separation. Also, due to the PEG's high saturation and paramagnetic behavior, it should be studied as a biosensor. PVA coating has been employed in various fields such as drug delivery as membranes for bone regeneration and other biomedical application. The results also indicated that by an increase in the temperature the magnetic saturation of the coated magnetic nanoparticles were increased. Furthermore, it is proved that for the PEG-coated Fe_3O_4 sample, the magnetic saturation and coercivity were about 60.98 emu g^{-1} and 8.26 G, respectively..

ACKNOWLEDGMENTS

The authors are thankful for the financial support of the Tehran North Branch at Islamic Azad University for analysis and discussions on the results.

REFERENCES

[1] Arosio, P., Applications and Properties of Magnetic Nanoparticles. *Nanomaterials*. **2021**, *11*, 1297-1300,

DOI: 10.3390/nano11051297.

[2] Ibrahim, P.; Saeed, k.; Khan, I., Nanoparticles: Properties, applications and toxicities. *Arab. J. Chem.* **2019**, *12*, 908-931, DOI: 10.1016/j.arabjc.2017.05.011.

[3] Monsalve, A.; Vicente, J.; Grippin, A.; Dobson, J., Poly (lactic acid) magnetic microparticle synthesis and surface functionalization. *IEEE Magn. Lett.* **2017**, *8*, 1-5, DOI: 10.1109/LMAG.2017.2726505.

[4] Bansal, R.; Gronkiewicz, B.; Storm, G.; Prakash, J., Relax in-coated superparamagnetic iron-oxide nanoparticles as a novel theragnostic approach for the diagnosis and treatment of liver fibrosis. *J. Hepatol*. **2017**, *66*, S43, DOI: 10.1016/S0168-8278(17)30348-3.

[5] Ali, A.; Zafar, H.; Zia, M.; Haq, I.; Phil, A. R.; Ali, J. S.; Hussain, A., Synthesis, characterization, applications, and challenges of iron oxide nanoparticles. *Nanotechnol. Sci. App*. **2016**, *9*, 49-67. DOI: 10.2147/NSA.S99986.

[6] Mohammed, L.; Gomaa, H. G.; Ragab, D.; Zhu, J., Magnetic nanoparticles for environmental and biomedical applications: a review. *Protistology*. **2017**, *30*, 1-14. DOI: 10.1016/j.partic.2016.06.001.

[7] Zhu, K.; Ju, Y.; Xu, J.; Yang, Z.; Gao, S.; Hou. Y., Magnetic nanomaterials: chemical design, synthesis and potential applications. *Acc Chem. Res*. **2018**, *51*, 404-413, DOI: 10.1021/acs.accounts.7b00407.

[8] Su, D.; Wu, K.; Krishna, V.; Klein, T.; Liu, J.; *et al*., Detection of influenza a virus in swine nasal swab samples with a wash-free magnetic bioassay and a handheld giant magnetoresistance sensing system. *Front. Microbiol.* **2019**, *10*, 1077. DOI: 10.3389/fmicb.2019.01077.

[9] Zhang, Q.; Yang, X.; Guan, J., Applications of Magnetic nanomaterials in heterogeneous catalysis. *ACS Appl. Nano Mater.* **2019**, *2*, 4681-4697, DOI: 10.1021/acsanm.9b00976.

[10] Wu, K.; Su, D.; Saha, R.; Wong, D.; Wang, J. P., Magnetic particle spectroscopy-based bioassays: methods, applications, advances, and future opportunities. *J. Phys. D: Appl. Phys.* **2019**, *52*, 173001, DOI: 10.1088/1361-6463/ab03c0.

[11] Wu, K.; Klein, T.; Krishna, V. D.; Su, D.; Perez, A. M.; Wang, J. P., Portable GMR handheld platform for the detection of influenza a virus. *ACS Sens.* **2017**, *2*, 1594-1601, DOI: 10.1021/acssensors.7b00432.

[12] Fish, M. B.; Fromen, C. A.; Lopez-Cazares, G.; Golinski, A. W.; Scott, T. F.; *et al*., Exploring deformable particles in vascular-targeted drug delivery: softer is only sometimes better. *Biomaterials*. **2017**, *124*, 169179. DOI: 10.1016/j.biomaterials.2017.02.002.

[13] Villanova, D.; Aponte, I.; Xiao, Z.; Colvin, V., Magnetic nanoparticles in biology and medicine: Past, present, and future trends. *Pharmaceutics*. **2021**, *13*, 943, DOI: 10.3390/pharmaceutics13070943.

[14] Dutz, S., Are magnetic multicore nanoparticles promising candidates for biomedical applications? *IEEE Trans. Magn*. **2016**, *52*, 0200103, DOI: 10.1109/TMAG.2016.2570745.

[15] Effenberger, F. B.; Couto, R. A.; Kiyohara, P. K.; Machado, G.; Masunaga, S. H., *et al*., Economically attractive route for the preparation of high-quality magnetic nanoparticles by the thermal decomposition of iron(III) acetylacetonate. *Nanotechnology*. **2017**, *28*, 115603. DOI: 10.1088/1361-6528/aa5ab0.

[16] Chen, F.; Xie, S.; Zhang, J.; Liu, R., Synthesis of spherical Fe_3O_4 magnetic nanoparticles by co-precipitation in choline chloride/urea deep eutectic solvent. *Mater. Lett.* **2013**, *112*, 177-179. DOI: 10.1016/j.matlet.2013.09.022.

[17] Patselas, V.; Kosinová, L.; Lovri, M.; Ferhatovic, L.; Rabyk, M.; *et al*., Superparamagnetic Fe_3O_4 nanoparticles: synthesis by thermal decomposition of iron(III) glucuronate and application in magnetic resonance imaging. *ACS Appl. Mater. Interfaces*. **2016**, *8*, 7238-7247. DOI: 10.1021/acsami.5b12720.

[18] Albert, E. L.; Che Abdullah, C. A.; Shirataki, Y., Synthesis and characterization of graphene oxide functionalized with magnetic nanoparticle *via* simple emulsion method. *Results Phys.* **2018**, *11*, 944-950. DOI: 10.1016/j.rinp.2018.10.054.

[19] Ali, A.; Rehmat, S.; Zhou, P.; Guo, M.; Ovais, M.; *et al*., Review on recent progress in magnetic nanoparticles: Synthesis, characterization, and

diverse applications. *Front Chem*. **2021**, *9*, 629054, DOI: 10.3389/fchem.2021.629054.

[20] Bajaj, N. S.; Joshi, R. A., Energy materials: synthesis and characterization techniques, in energy mater. **2021**, 61-82, DOI: 10.1016/B978-0-12-823710-6.00019-4.

[21] Koo, K.; Ismail, A. E.; Othman, M. D.; Bidin, N.; Rahman, M., Preparation and characterization of superparamagnetic magnetite (Fe_3O_4) nanoparticles: A short review. *Malaysian J. Fund. Appl. Sci.* **2019**, *15*, 23-31. DOI: 10.11113/mjfas.v15n2019.1224.

[22] Yeap, S. P.; Lim, L. K.; Ooi, B. S.; Ahmad, A. A., Agglomeration, colloidal stability, and magnetic separation of magnetic nanoparticles: collective influences on environmental engineering applications. *J. Nanoparticle. Res.* **2017**, *19*, 368, DOI: 10.1007/s11051-017-4065-6.

[23] Ahrberg, C. D.; Choi, J. W.; Chung, B. G., Automated droplet reactor for the synthesis of iron oxide/gold core-shell nanoparticles. *Sci. Rep*. **2020**, *10*, 1737. DOI: 10.1038/s41598-020-58580-9.

[24] Salehipour, M.; Rezaei, S.; safer, J.; Pakdin-Parizi, Z., Recent advances in polymer-coated iron oxide nanoparticles as magnetic resonance imaging contrast agents. *J. Nanoparticle Res*. **2021**, *23*, DOI: 10.1007/s11051-021-05156-x.

[25] Liu, B.; Wang, D.; Huang, W.; Yao, A.; Kamitakahara, M.; Ioku, K., Preparation of magnetite nanoparticles coated with silica *via* a sol-gel approach. *J. Ceram. Soc. Japan*. **2007**, *115*, 877-881. DOI: 10.2109/jcersj2.115.877.

[26] Wei, Y.; Han, B.; Hu, X., Lin, Y.; Wang, X.; Deng, X., Synthesis of Fe_3O_4 nanoparticles and their magnetic properties. *Procedia Eng.* **2012**, *27*, 632-637. DOI: 10.1016/j.proeng.2011.12.498.

[27] Karimzadeh, I.; Aghazadeh, M.; Davoudi, T.; Ganjali, M. R.; Koliva, P. H., Superparamagnetic iron oxide (Fe_3O_4) nanoparticles coated with PEG/PEI for biomedical applications: A facile and scalable preparation route based on the cathodic electrochemical deposition method. *Adv. Phys. Chem.* **2017**, 9437487, DOI: 10.1155/2017/9437487.

[28] Anil, A. C.; Govindan, K.; Rangarajan, M., Synthesis of poly (ethylene glycol) (PEG)-capped Fe_3O_4 nanoclusters by hydrothermal method. IOP Conf. Ser.: *Mater. Sci. Eng*. **2019**, *577*, 012153, DOI: 1757-899X/577/1/012153.

[29] Ulfa, M.; Prasetyoko, D.; Bahruji, H.; Nugraha, R. E., Green synthesis of hexagonal hematite (α-Fe_2O_3) flakes using pluronic F127-Gelatin template for adsorption and photodegradation of ibuprofen. *Materials*, **2021**, *14*, 6779, DOI: 10.3390/ma14226779.

[30] Antarnusa, G.; Suharyadi, E., A synthesis of polyethylene glycol (PEG)-coated magnetite Fe_3O_4 nanoparticles and their characteristics for enhancement of biosensor. *Mater. Res. Express.* **2020**, *7*, 056103, DOI: 10.1088/2053-1591/ab8bef.

[31] Farahmandjou, M.; Salehizadeh, S.A., The optical band gap and the tailing states determination in glasses of TeO_2-V_2O_5-K_2O system. *Glass. Phys. Chem.* **2013**, *39*, 473-479, DOI: 10.1134/S1087659613050052.

[32] Maleki, A.; Niksefat, M.; Rahimi, J.; Hajizade, Z., Design and preparation of Fe_3O_4@PVA polymeric magnetic nanocomposite film and surface coating by sulfonic acid *via in situ* methods and evaluation of its catalytic performance in the synthesis of dihydropyridines. *BMC Chem*. **2019**, *19*, DOI: 10.1186/s13065-019-0538-2.

[33] Scherrer, P., Bestimmung der inneren Struktur und der Größe von Kolloidteilchen mittels Röntgenstrahlen. Kolloidchemie Ein Lehrbuch. *Springer, Berlin, Heidelberg,* **1912**, 387-409, DOI: 10.1007/978-3-662-33915-2_7.

[34] Farahmandjou, M.; Motaghi, S., Sol-gel Synthesis of Ce-doped α-Al_2O_3: Study of Crystal and Optoelectronic Properties. *Opt. Commun*. **2019**, *441*, 1-7, DOI: 10.1016/j.optcom.2019.02.029.

[35] Farahmandjou, M.; Jurablu, S., Co-Precipitation Synthesis of Zinc Oxide (ZnO) Nanoparticles by Zinc Nitrate Precursor. *Int. J. Bio-Inorg. Hybr. Nanomater.* **2014**, *3*, 179-184.

[36] Assay, F.; Jafarizadeh-Malamiri, H.; Ajman, Anarjan, N.; Vaghari, H.; *et al*., A biotechnological perspective on the application of iron oxide nanoparticles. *Nano Res.* **2016**, *9*, 2203-2225, DOI: 10.1007/s12274-016-1131-9.

[37] Shokrollahi, H., A review of the magnetic properties, synthesis methods and applications of maghemite. *J. Magnet. Mater.* **2017**, *426*, 74-81, DOI: 10.1016/j.jmmm.2016.11.033.

[38] Khodadadi, A.; Farahmandjou, M.; Yaghoubi, M., Investigation on synthesis and characterization of Fe-doped Al_2O_3 nanocrystals by new sol-gel precursors. *Mater. Res. Express.* **2018**, *6*, 025029, DOI: 10.1088/2053-1591/aaef70.

[39] Eskandari, M. J.; Hasanzadeh, I., Size-controlled synthesis of Fe_3O_4 magnetic nanoparticles *via* an alternating magnetic field and ultrasonic-assisted chemical co-precipitation, *Mat. Sci. Eng. B* **2021**, *266*, 115050, DOI: 10.1016/j.mseb.2021.115050.

[40] Rezazadeh, L.; Sharafi, S.; Schaffie, M., Application of oxidation-reduction potential (ORP) as a controlling parameter during the synthesis of Fe_3O_4@PVA nanocomposites from industrial waste (raffinate). *Environ. Sci. Pollut. Res.* **2020**, *27*, 32088-3209 DOI: 10.1007/s11356-020-09436-2.

[41] Janani, B.; Al-Mohaimeed, A. M.; Raju, L. L., Synthesis and characterizations of hybrid PEG-Fe_3O_4 nanoparticles for the efficient adsorptive removal of dye and antibacterial, and antibiofilm applications. *J. Environ. Health. Sci. Eng.* **2021**, *19*, 389-400, DOI: 10.1007/s40201-021-00612-1.

[42] Zarinkamar, M.; Farahmandjou, M.; Pourmirjafari, F.T., Diethylene glycol-mediated synthesis of nano-sized ceria (CeO_2) catalyst. *J. Nanostruct.* **2016**, *6*, 116-120, DOI: 10.7508/jns.2016.02.002.

[43] Ganesha, A.; Denny, Y.R.; Suherman, A.; Utami, I. S.; Saefullah, A., The effect of additional polyethylene glycol (PEG) as coating Fe_3O_4 for magnetic nanofluid applications. *Recent Innov. Chem. Eng.* **2021**, *14*, 335-346, DOI: 10.2174/2405520414666210325122511.

[44] Hayashi, K.; Tomonaga, H.; Matsuyama, T.; Ida, J., Facile synthesis, characterization of various polymer immobilized on magnetite nanoparticles applying the coprecipitation method, *J. Appl. Polym. Sci.* **2022**, *139*, 51581, DOI: 10.1002/app.51581.